



## NIH PUBLIC ACCESS

## Author Manuscript

*J Surg Res.* Author manuscript; available in PMC 2008 August 1.

Published in final edited form as:

*J Surg Res.* 2007 August ; 141(2): 134–140.

## Detection and Characterization of Hepatic Engraftment of Embryonic Stem Derived Cells by Fluorescent Stereomicroscopy

Montserrat Caballero, Ph.D.<sup>1</sup>, Harry M. Lightfoot Jr., M.D.<sup>1</sup>, Michael LaPaglia, M.D.<sup>1</sup>, Andrew Pleasant, B.S.<sup>1</sup>, Seigo Hatada, Ph.D.<sup>2</sup>, Bruce A. Cairns, M.D.<sup>1,\*</sup>, and Jeffrey H. Fair, M.D.<sup>1,\*</sup>

<sup>1</sup>Department of Surgery, University of North Carolina at Chapel Hill, North Carolina, USA

<sup>2</sup>Department of Pathology and Laboratory Medicine, University of North Carolina at Chapel Hill, North Carolina, USA

### Abstract

**Background**—Embryonic Stem (ES) cells have been investigated as a potential replacement therapy for failed organs, such as the liver. However, detection of hepatic engraftment from candidate stem cells has been difficult due to low engraftment efficiency. Previous detection methods required that the graft be processed by molecular and/or immunohistochemical techniques, limiting further functional studies. This study evaluated the use of tri-dimensional (3-D) fluorescent stereomicroscopy for gross detection of ES cell derived hepatic engraftment.

**Material and methods**—Murine ES cells expressing the enhanced green fluorescence protein (EGFP) underwent directed endodermal lineage differentiation. Three days after 2/3rds partial hepatectomy, cells were injected into the liver parenchyma, and livers were harvested at 10–20 days and examined by fluorescence stereomicroscopy with a GFP2 long pass filter. The sensitivity and reliability of the test was evaluated using quantitative PCR to assay for the presence of EGFP mRNA in the tissue.

**Results**—Fluorescent microscopy detected EGFP-positive cells engrafted with normal histology in 5 of 11 specimens. EGFP mRNA was confirmed in all five specimens by q-PCR. Only 1 of the 11 specimens was negative by fluorescence stereomicroscopy and positive by q-PCR,  $P < 0.02$ , Fisher's exact test.

**Conclusion**—Utilization of 3-D stereomicroscopy with a GFP2 long pass filter is a powerful and fast screening tool for GFP-ES derived hepatic engraftment.

### Keywords

Embryonic stem cells; liver; transplant; fluorescence; stereomicroscopy; engraftment efficiency

## INTRODUCTION

The insufficient availability of donor organs for liver transplantation has increased the requirement for new alternative therapies for end stage liver disease. One of these potential new therapies, cellular transplantation, is being intensively investigated and is based in part on

Corresponding Author: Montserrat Caballero, **Address:** 2110 Bioinformatics Bldg. CB# 7211, Chapel Hill, NC 27599-7211, **Phone:** (919) 843-1804, **Fax:** (919) 966-6308, **Email:** [Montserrat\\_Caballero@med.unc.edu](mailto:Montserrat_Caballero@med.unc.edu).

\*These authors are co-senior authors for the paper.

**Publisher's Disclaimer:** This is a PDF file of an unedited manuscript that has been accepted for publication. As a service to our customers we are providing this early version of the manuscript. The manuscript will undergo copyediting, typesetting, and review of the resulting proof before it is published in its final citable form. Please note that during the production process errors may be discovered which could affect the content, and all legal disclaimers that apply to the journal pertain.

the liver's regenerative nature. Numerous animal studies have shown the ability of mature hepatocytes to repopulate acutely damaged livers [1] [2] [3] and mature hepatocytes have been used clinically with some success [4] [5]. However, these cells demonstrate significant limitations, such as limited repopulation capability and allograft rejection [6]. Due to these problems, other laboratories, including ours, have done studies with phenotypically defined hepatic progenitors as candidates for cell transplantation [7-9]. Although the hepatic progenitor appeared to be a good candidate due to its stem cell characteristics, it has been proven to be difficult to isolate [7]. As an alternative, the use of embryonic stem (ES) cell derivatives is particularly attractive, because of their ability to be expanded in culture, their plasticity [10-12] and the subsequent potential to undergo directed differentiation under appropriate *in vitro* conditions [13,14]. An additional theoretical advantage of ES cells is their expected immune privilege [15].

While promising, the embryonic stem cell derivatives have shown a low engraftment efficiency, lack of function in the liver [16] [17], and even fusion of the injected cells to the surrounding hepatocytes [18]. Therefore, a more direct approach based on the developmental relationship between ES cells, definitive endoderm and hepatocellular function is required in order to increase efficiency, function and safety of ES cell derivative transplants into the liver. Our lab had recently shown that ES cells differentiate into putative endodermal precursors (PEPs) after direct differentiation *in vitro* in the presence of acidic fibroblast growth factor (aFGF). We have been able to deliver these PEPs into the liver parenchyma, resulting in high engraftment efficiency, and we have also been able to show recovery of function in both a syngeneic and allogeneic model in a Factor-IX (F-IX) Knockout (KO) murine model. In addition, we performed genetic analysis on laser capture microdissected PEPs from the engrafted areas that excluded cell fusion as the main engraftment mechanism [19].

There are still several open questions that need to be addressed regarding the efficiency and safety issue. Multiple variables can be modified *in vitro* in order to affect the degree of ES cell differentiation into the desired lineage pre-transplantation [20-22] that may also affect the engraftment efficiency, liver regeneration and recovery of function. Additionally, some of these modifications may also result in the decrease of spontaneous differentiation into undesirable lineages and substantial reduction of the risk of teratoma formation [22,23]. The ability to track the ultimate *in vivo* effect of the *in vitro* variables requires an accurate, high throughput model in which the engraftment characteristics can be detected.

Previous studies of engraftment efficiency have used several molecular and immunohistochemical methods including: flow cytometry [24-28], histological and immunostaining techniques [28-30], b-gal staining analysis of whole liver and tissue sections [31], different types of PCR analysis [32-35] and/or a combination of several of these methods [36]. As the use of such methods has proven to be labor intensive and costly, we examined past attempts at detection and evaluation of cellular structural function and liver sinusoidal architecture to determine if similar strategies could be applied to our models. Most of these characterizations have taken advantage of the use of different microscopy techniques to evaluate structure and function [37-39]. In addition, 3-D microscopy has been successfully applied to the detection of fluorescence cells in large specimens [40-42]. Thus, we have applied this microscopy technique in a novel way to study engraftment levels in our model.

In this paper we describe an improved method for preliminary gross detection of engrafted areas within the liver using genetically labeled fluorescent ES cells and 3-D fluorescent stereomicroscopy. The use of stereomicroscopy has shown to be extremely useful and critical in identifying samples that demonstrate positive engraftment and allows us to efficiently focus on detailed characterization only on samples that show positivity [19].

## MATERIALS AND METHODS

### Cell Culture

The murine ES cells, A129Bk4 (elf), express the enhanced GFP fused to a nuclear targeting tag, driven by the b-actin promoter [13]. ES cells were propagated over fibroblast feeder layers and differentiated in collagen plates in the presence of 100 ng/ml of aFGF as described previously [19]. At 7 days post-differentiation, cells were harvested, re-suspended at  $1 \times 10^4$  cells/ $\mu$ l in 1% FBS-PBS, and injected into mice.

### Animal Model

A total of 11 males, ages 8 to 16 -week-old BALB/c, C57BL/6 and F-IX deficient mice were used in this study. Wild types were obtained from the Jackson Laboratories (Bar Harbor, ME) and F-IX knockouts from Dr. Darrell Stafford of the Department of Biology (University of North Carolina at Chapel Hill, NC). Animals were maintained in a controlled environment and the facility is managed by the Division of Laboratory Animal Management (DLAM), Chapel Hill, NC.

### Surgical Procedures

All surgical procedures were performed in accordance with protocols approved by the Institute of Animal Care and Use Committee (IACUC). Mice were subjected to 2/3rds partial hepatectomy as described by Higgins and Anderson [43] under anesthesia (60mg/kg ketamine; 6 mg/kg xylazene). Two days after partial hepatectomy, 100  $\mu$ l of differentiated ES cells were injected into the liver parenchyma at a density of  $10^4$  cells/ $\mu$ l. The ES cell dose was chosen based on previously published data for hepatocyte transplantation (revised on [44]) To perform the partial hepatectomy on the F-IX KO mice, the mice were given 100 units/kg recombinant human F-IX (from the laboratory of Dr. Stafford) [45], both by intramuscular and subcutaneous injection after anesthesia, and another dose 4 hours (h) after the operation. At the time when the GFP-PEP injections were performed on postoperative day 3, the intramuscular and subcutaneous doses of human F-IX were repeated. Recombinant human F-IX (stock concentration: 575  $\mu$ g/ml) was used.

### Fluorescent Stereomicroscopy

In order to identify the engraftment, mice were sacrificed 10 to 20 days after transplantation and the liver was harvested. Fresh liver samples were then examined with a stereomicroscope (MZ16FA; Leica Microsystems AG, Wetzlar, Germany) with the GFP2 long pass filter (100447084, Leica Microsystems AG, Wetzlar, Germany) for the presence of GFP positive cells.

### Histological Analysis

To further characterize cell engraftment, liver tissue samples were washed in phosphate buffer (PBS), fixed overnight in 4% paraformaldehyde and processed for cryosectioning [19]. Tissue samples were analyzed by standard fluorescent microscopy (Axiovert S100; Carl Zeiss MicroImaging, Inc., Thornwood, NY).

### Immunofluorescence

Slides with tissue cryosections processed as above were washed twice in PBS, permeabilized, and blocked against nonspecific binding in blocking buffer (5% normal serum/2% BSA/0.1% Triton X-100 in PBS) for 30 minutes (min). Samples were then incubated with sheep anti-rat F-IX antibody (Haematologic Technologies, Essex Junction, VT) for 90 min at room temperature at a final dilution of 1:200 in blocking buffer. After the incubation, samples were washed three times with PBS-0.05% Triton X-100, followed by incubation with Texas red-

labeled anti-sheep IG (Fab'2) IgG (Jackson ImmunoResearch Laboratories, West Grove, PA) diluted 1:200 in blocking buffer for 30 min. After three washings in PBS-0.1% Triton X-100, samples were incubated with rabbit polyclonal GFP antibody conjugated to Alexa Fluor 488 (Molecular Probes) for 1 h at room temperature (1:400 dilution in blocking buffer). After three washings with PBS-0.1% Triton X-100, they were mounted with Vectashield mounting media (Vector Laboratories). This last procedure was also used for the samples that were only incubated with anti -GFP antibody conjugated to Alexa Fluor 488. Processed slides were examined under a Zeiss Axiovert S100 fluorescent microscope, and representative slides were further analyzed by a confocal laser-scanning microscopy performed on a Zeiss LSM5 Pascal microscope (Thornwood, NY).

### PCR Analysis

Quantitative RT-PCR analysis was used to confirm the presence of GFP mRNA. The cDNA was synthesized by oligo-dT priming and subjected to PCR amplification with primer sets for EGFP and b-actin for internal control. PCR was performed in a total reaction volume of 50 µl consisting of 1 µM each primer, 200 µM dNTP, 50 mM KCl, 1.5 mM MgCl<sub>2</sub>, 10 mM Tris HCl, pH 8.3 and 1.2 U Amplitaq polymerase (Cetus Corporation, Berkeley, CA). Samples were denatured at 94°C for 3 min followed by 30 amplification cycles (1 min at 94 °C, 1 min at 62°C and 2 min at 72 °C) and a final extension at 72 °C for 5 min. Samples were analyzed in 2% agarose gel in Tris/Acetate/EDTA buffer and visualized with ethidium bromide. The primers used for EGFP detection by RT-PCR were: 5'aca aca gcc aca acg tct ata as forward primer and 5'gtg gcg gat ctt gaa gtt ca as the reverse primer.

### Statistical Analysis

Data was obtained from direct observation under the 3-D microscope and compared to the RT-PCR. The Fisher's exact test was used for statistical analysis.

## RESULTS

The 11 mice, 6 transplanted with PEPs and 5 non-transplanted controls, were sacrificed between days 10 to 20 after ES derived cells were injected into the liver parenchyma of experimental models and the livers were harvested for examination by fluorescent stereomicroscopy and qRT-PCR analysis. Fresh livers were analyzed by 3-D fluorescent stereomicroscopic observation and positive fluorescent cells were detected in 5 of the 6 samples from the transplanted mice. Fluorescence above the general background was not detected in one of the samples from the transplanted mice or in any of the five control samples. In Figure 1 representative results from one of the samples analyzed 10 days post injection are shown. Clear fluorescent patches can be readily detected in the liver surface (a, b). At higher magnification the fluorescent patches can be identified as clusters of GFP positive cells (c, d) embedded in the liver parenchyma. Representative histological studies of this same sample are shown in Figure 2. ES derived cell engraftment can be detected and identified in the tissue section by the nuclear localization of the GFP.

To confirm the presence of GFP and further characterize the engrafted cells' morphology within the liver architecture, representative tissue samples were analyzed by immunofluorescence techniques using a specific GFP antibody. As it is shown in Figure 3, this study demonstrates the presence of GFP positive cells with different morphological characteristics embedded in the liver parenchyma. Both cells exhibit a clear distinct morphology (a, b) and cells similar to the surrounding cells, can be detected in the engrafted areas (c, d).

As part of the engrafted cells' characterization, liver samples from F-IX KO injected mice were analyzed by stereomicroscopy and positive areas were subjected to immunofluorescence characterization using both anti-FIX and anti-GFP antibody. Figure 4 shows a representative picture demonstrating that the GFP + cell (b) and F-IX (c) cell are in the same engrafted area. The overlay image (d) showing co-localization seems to indicate that some of the cells may have become hepatocytes, as only hepatocytes have been described to produce F-IX.

In order to evaluate the sensitivity and reliability of the gross detection by fluorescent stereomicroscopy, we analyzed tissue samples from the fresh liver for the presence of GFP mRNA by qRT-PCR. Although only 5 out of 6 samples from transplanted mice were positive by fluorescence and all of them were positive for GFP when assayed by qRT-PCR. The other 5 control samples that were fluorescence negative were also negative by qRT-PCR (Table 1).

## DISCUSSION

We have previously used different techniques for the analysis of engraftment efficiency, including: flow cytometry, PCR and histological analysis. All of them have significant time and cost issues as our research requires the analysis of a large number of samples from each individual mouse of which only a small percentage demonstrated positive engraftment. Thus, we have created an innovative, cost-effective, and time-saving method for preliminary gross detection of engrafted areas within the liver.

A fluorescent stereomicroscope equipped with GFP filter allows for direct observation of fluorescence without any tissue treatment. In this study clusters of engrafted cells in the surface of the liver are easily detectable. Use of the appropriate observation filters, such as the GFP2 long pass filter together with the nuclear localization of the GFP, generates an image that easily discriminates between real positive engraftment and the general autofluorescence produced by the liver. These observations were validated by a good correlation between the observation of fluorescence and detection of GFP positive cells by qRT-PCR and histological analysis.

As described in the Results section, the technique identified positive engraftment in 5 out of the 6 samples obtained from transplanted animals; all of them tested positive for engraftment when analyzed by RT-PCR. As we do not have the engraftment efficiency in those samples, we do not know if the fluorescence-negative samples had only a very small limited engraftment that could only be detected by a more sensitive technique such as PCR (Table 1); Alternatively the engrafted area could have been located more internally and would not be accessible to the penetration range of the stereomicroscope. Although the sensitivity of the technique is 83% while the PCR is 100%, the specificity is 100% with no fluorescence detected in any of the negative control samples. We can therefore conclude that the utilization of 3-D fluorescent stereomicroscopy provides a fast, sensitive and reliable tool to define which sample tissues have engrafted.

In addition, identification by stereomicroscopy of these specific engrafted areas within the liver sample is crucial for characterization by immunostaining. Stereomicroscopy demonstrated that GFP positive engrafted cells acquire hepatic morphology and are able to synthesize F-IX in our hemophilic mouse models. We were also able to retrieve GFP positive cells from the best engrafted areas by LCM for genetic analysis. The results of the genomic DNA contribution analysis show no detectable co-localization of wild type DNA with GFP DNA in the fluorescence positive areas of the liver parenchyma, thus excluding cell fusion as the main engraftment mechanism in our models [19]. The use of 3-D microscopy has also been an important tool for characterization of the liver parenchyma, with special interest in areas of positive engraftment that showed the presence of ES derived cells with different morphologies. These morphologies may correspond with different cellular states. Alternately, the large cells

with distinct morphology may represent cell types other than those derived from the endoderm or cells that are not able to integrate within the tissue and demonstrate senescence with time. On the contrary, GFP+ cells in other engrafted areas with morphology similar to that of the surrounding hepatocytes could be observed. Some of those ES derived cells are able to function as hepatocytes as indicated by the presence of F-IX, co-localizing with GFP+ cells in the transplanted F-IX KO mice liver samples. The histological characterization of positive engrafted areas also showed no morphological evidence of immunological rejection.

As a further step to expand the relevance of the engraftment evaluation by fluorescence stereomicroscopy, our laboratory is currently using this technique to compare the effect of different surgical procedures on the ES cells engraftment efficiency. Quantitative analysis of engraftment efficiency by PCR is studied in parallel with qualitative analysis of engraftment localization analyzed by fluorescence stereomicroscopy, as described in this publication.

In conclusion, the present study revealed that scanning the sample by fluorescence stereomicroscopy is a powerful and reliable tool for fast screening of EGFP-ES derived hepatic engraftment areas in the liver of transplanted mice. The use of this technique in detecting positive engraftment showed that PEPs are able to engraft in the liver parenchyma without fusion to the surrounding hepatocytes and that they acquire both hepatic morphology and function shown by the production of F-IX. This study has been made in both syngeneic and allogeneic models without any evidence of rejection and has been reported in Proceedings of the National Academy of Sciences [19].

#### Acknowledgements

Funding supported by the National Institutes of Health: K18 DK065013 (J.H.F.) and K08 GM 067147 (B.A.C.); the North Carolina Jaycee Burn Center; Astellas Pharma, Inc. and the University Research Council's Small Grants Program.

#### References

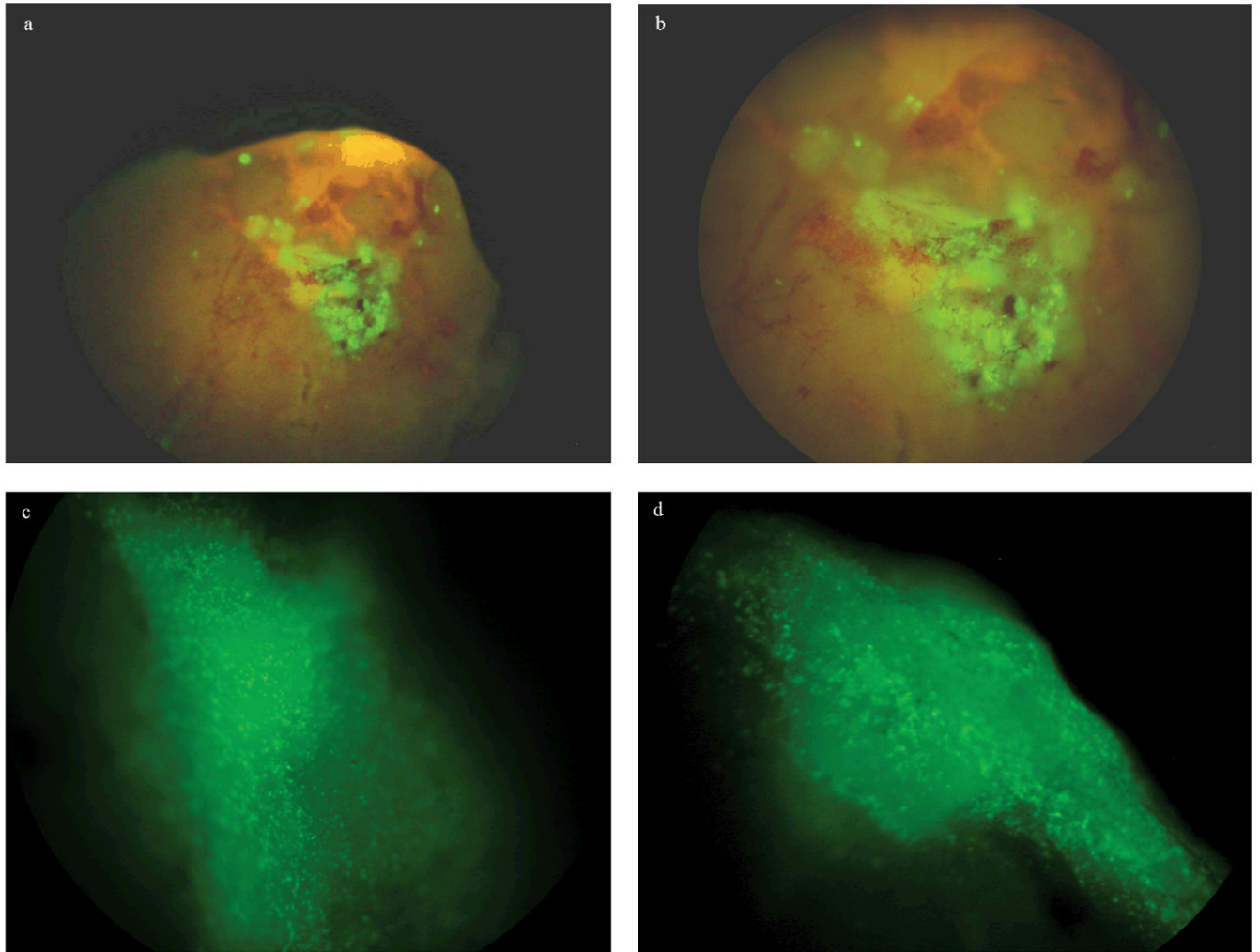
1. Gupta S, Bhargava KK, Novikoff PM. Mechanisms of cell engraftment during liver repopulation with hepatocyte transplantation. *Semin Liver Dis* 1999;19(1):15–26. [PubMed: 10349680]
2. Gupta S, Gorla GR, Irani AN. Hepatocyte transplantation: emerging insights into mechanisms of liver repopulation and their relevance to potential therapies. *J Hepatol* 1999;30(1):162–70. [PubMed: 9927165]
3. Strom S, Fisher R. Hepatocyte transplantation: new possibilities for therapy. *Gastroenterology* 2003;124(2):568–71. [PubMed: 12557161]
4. Bilir BM, et al. Hepatocyte transplantation in acute liver failure. *Liver Transpl* 2000;6(1):32–40. [PubMed: 10648575]
5. Strom SC, et al. Hepatocyte transplantation as a bridge to orthotopic liver transplantation in terminal liver failure. *Transplantation* 1997;63(4):559–69. [PubMed: 9047152]
6. Bumgardner GL, Orosz CG. Unusual patterns of alloimmunity evoked by allogeneic liver parenchymal cells. *Immunol Rev* 2000;174:260–79. [PubMed: 10807522]
7. Susick R, et al. Hepatic progenitors and strategies for liver cell therapies. *Ann N Y Acad Sci* 2001;944:398–419. [PubMed: 11797689]
8. Sadiq TS, Gerber DA. Stem cells in modern medicine: reality or myth? *J Surg Res* 2004;122(2):280–91. [PubMed: 15555629]
9. Kubota H, Reid LM. Clonogenic hepatoblasts, common precursors for hepatocytic and biliary lineages, are lacking classical major histocompatibility complex class I antigen. *Proc Natl Acad Sci U S A* 2000;97(22):12132–7. [PubMed: 11050242]
10. Edwards RG. Stem cells today: A. Origin and potential of embryo stem cells. *Reprod Biomed Online* 2004;8(3):275–306. [PubMed: 15038895]
11. Itskovitz-Eldor J, et al. Differentiation of human embryonic stem cells into embryoid bodies compromising the three embryonic germ layers. *Mol Med* 2000;6(2):88–95. [PubMed: 10859025]



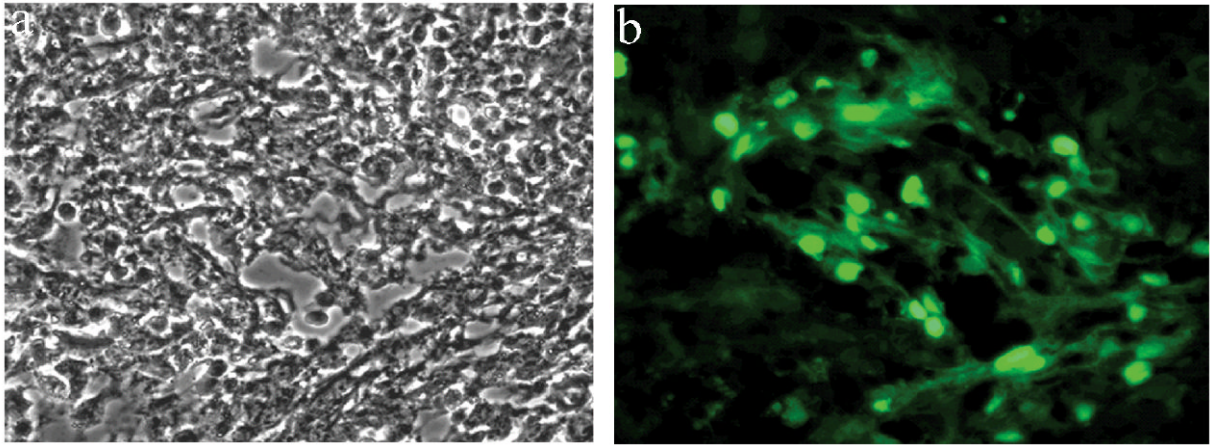
12. Odorico JS, Kaufman DS, Thomson JA. Multilineage differentiation from human embryonic stem cell lines. *Stem Cells* (Dayton, Ohio) 2001;19(3):193–204.
13. Fair JH, et al. Induction of hepatic differentiation in embryonic stem cells by co-culture with embryonic cardiac mesoderm. *Surgery* 2003;134(2):189–96. [PubMed: 12947317]
14. Hamazaki T, et al. Hepatic maturation in differentiating embryonic stem cells in vitro. *FEBS Lett* 2001;497(1):15–9. [PubMed: 11376655]
15. Drukker M, et al. Characterization of the expression of MHC proteins in human embryonic stem cells. *Proc Natl Acad Sci U S A* 2002;99(15):9864–9. [PubMed: 12114532]Epub 2002 Jul 11
16. Yamada T, et al. In vitro differentiation of embryonic stem cells into hepatocyte-like cells identified by cellular uptake of indocyanine green. *Stem Cells* 2002;20(2):146–54. [PubMed: 11897871]
17. Yin Y, et al. AFP(+), ESC-derived cells engraft and differentiate into hepatocytes in vivo. *Stem Cells* 2002;20(4):338–46. [PubMed: 12110703]
18. Terada N, et al. Bone marrow cells adopt the phenotype of other cells by spontaneous cell fusion. *Nature* 2002;416(6880):542–5. [PubMed: 11932747]Epub 2002 Mar 13
19. Fair JH, et al. Correction of factor IX deficiency in mice by embryonic stem cells differentiated in vitro. *Proc Natl Acad Sci U S A* 2005;102(8):2958–63. [PubMed: 15699326]Epub 2005 Feb 7
20. Czyz J, Wobus A. Embryonic stem cell differentiation: the role of extracellular factors. *Differentiation* 2001;68(45):167–74. [PubMed: 11776469]
21. Kanda S, et al. In vitro differentiation of hepatocyte-like cells from embryonic stem cells promoted by gene transfer of hepatocyte nuclear factor 3 beta. *Hepatol Res* 2003;26(3):225–231. [PubMed: 12850695]
22. Menard C, et al. Cardiac specification of embryonic stem cells. *J Cell Biochem* 2004;93(4):681–687. [PubMed: 15389971]
23. Bieberich E, et al. Selective apoptosis of pluripotent mouse and human stem cells by novel ceramide analogues prevents teratoma formation and enriches for neural precursors in ES cell-derived neural transplants. *J Cell Biol* 2004;15:15.
24. Chute JP, et al. Quantitative analysis demonstrates expansion of SCID-repopulating cells and increased engraftment capacity in human cord blood following ex vivo culture with human brain endothelial cells. *Stem Cells* 2004;22(2):202–15. [PubMed: 14990859]
25. Taylor PA, et al. Allogeneic fetal liver cells have a distinct competitive engraftment advantage over adult bone marrow cells when infused into fetal as compared with adult severe combined immunodeficient recipients. *Blood* 2002;99(5):1870–2. [PubMed: 11861310]
26. Schoeberlein A, et al. In utero transplantation of autologous and allogeneic fetal liver stem cells in ovine fetuses. *Am J Obstet Gynecol* 2004;191(3):1030–6. [PubMed: 15467585]
27. Koka PS, Kitchen CM, Reddy ST. Targeting c-Mpl for revival of human immunodeficiency virus type 1-induced hematopoietic inhibition when CD34+ progenitor cells are re-engrafted into a fresh stromal microenvironment in vivo. *J Virol* 2004;78(20):11385–92. [PubMed: 15452260]
28. Fandrich F, et al. Preimplantation-stage stem cells induce long-term allogeneic graft acceptance without supplementary host conditioning. *Nat Med* 2002;8(2):171–8. [PubMed: 11821902]
29. Grassi A, et al. Detection of recipient's cells in liver graft using antibodies to mismatched HLA class I antigens. *Liver Transpl* 2004;10(11):1406–14. [PubMed: 15497144]
30. Ise H, et al. Effective hepatocyte transplantation using rat hepatocytes with low asialoglycoprotein receptor expression. *Am J Pathol* 2004;165(2):501–10. [PubMed: 15277224]
31. Guo D, et al. Liver repopulation after cell transplantation in mice treated with retrorsine and carbon tetrachloride. *Transplantation* 2002;73(11):1818–24. [PubMed: 12085007]
32. Funkhouser AW, Vahed S, Soriano HE. A “real time” PCR assay to detect transplanted human liver cells in RAG-1<sup>-/-</sup> mice. *Cell Transplant* 2001;10(1):91–9. [PubMed: 11294476]
33. Wang LJ, et al. Engraftment assessment in human and mouse liver tissue after sex-mismatched liver cell transplantation by real-time quantitative PCR for Y chromosome sequences. *Liver Transpl* 2002;8(9):822–8. [PubMed: 12200785]
34. Song S, et al. Ex vivo transduced liver progenitor cells as a platform for gene therapy in mice. *Hepatology* 2004;40(4):918–24. [PubMed: 15382177]

35. Mas VR, et al. Engraftment measurement in human liver tissue after liver cell transplantation by short tandem repeats analysis. *Cell Transplant* 2004;13(3):231–6. [PubMed: 15191160]
36. Di Campi C, et al. A human umbilical cord stem cell rescue therapy in a murine model of toxic liver injury. *Dig Liver Dis* 2004;36(9):603–13. [PubMed: 15460845]
37. Nagai T, et al. Actin filaments around endothelial fenestrae in rat hepatic sinusoidal endothelial cells. *Med Electron Microsc* 2004;37(4):252–5. [PubMed: 15614450]
38. Laemmel E, et al. Fibered confocal fluorescence microscopy (Cell-viZio) facilitates extended imaging in the field of microcirculation. A comparison with intravital microscopy. *J Vasc Res* 2004;41(5):400–11. [PubMed: 15467299]Epub 2004 Sep 30
39. Melling M, et al. 3-D morphological characterization of the liver parenchyma by atomic force microscopy and by scanning electron microscopy. *Microsc Res Tech* 2004;64(1):1–9. [PubMed: 15287013]
40. Panoskaltis-Mortari A, et al. In vivo imaging of graft-versus-host-disease in mice. *Blood* 2004;103(9):3590–8. [PubMed: 14715632]Epub 2004 Jan 8
41. Yoshimoto M, et al. Direct visualization of transplanted hematopoietic cell reconstitution in intact mouse organs indicates the presence of a niche. *Exp Hematol* 2003;31(8):733–40. [PubMed: 12901979]
42. Chaudhuri TR, et al. A non-invasive approach for monitoring breast tumor cells during therapeutic intervention. *Cancer Biother Radiopharm* 2002;17(2):205–12. [PubMed: 12030114]
43. Higgins GM, A R. Experimental pathology of liver; restoration of liver of white rat following partial surgical removal. *Arch Pathol* 1931;12:186–2002.
44. Horslen SP, Fox IJ. Hepatocyte transplantation. *Transplantation* 2004;77(10):1481–6. [PubMed: 15239608]
45. Ahmad SS, et al. The role of the second growth-factor domain of human factor IXa in binding to platelets and in factor-X activation. *Biochem J* 1995;310(Pt 2):427–31. [PubMed: 7654178]

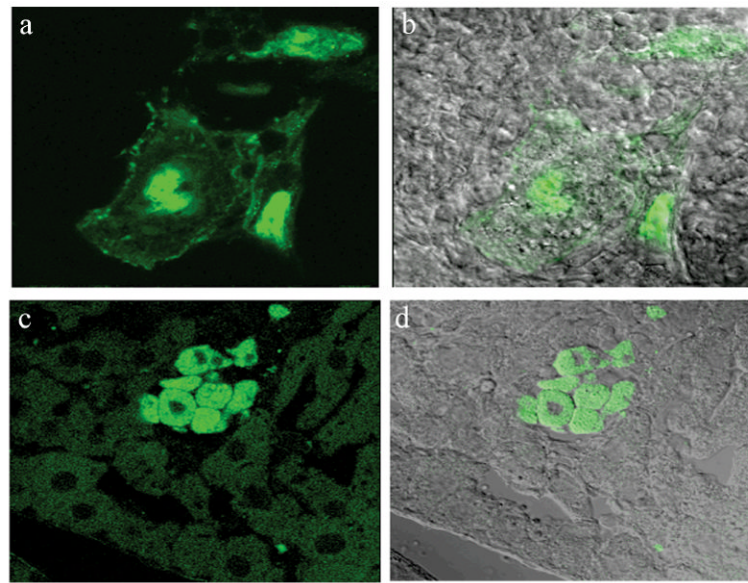




**Fig 1.** Fluorescence stereomicroscopic analysis of liver samples. .Representative images of engrafted areas on freshly dissected liver samples at 10 days post injection. Fluorescence patches can be detected at low magnification (a, b); higher magnification shows that these patches are formed by clusters of GFP positive cells (c, d).



**Fig 2.** Histological analysis of fluorescence patches. After dissection of fluorescent areas under fluorescence stereomicroscopic observation, the tissue was cryosectioned and subjected to (a) light and (b) fluorescence microscopic observation. The engrafted cells can be readily identified by the nuclear localization of the GFP.

**Fig 3.**

Immunofluorescence analysis of fluorescent positive areas. Fluorescent positive areas were cryosectioned, immunostained with anti-GFP antibody and fluorescence was analyzed by confocal microscopy, (a, c) fluorescence, (b, d) overlay with light analysis image. Antibody specific staining allows the identification of cells that lost their fluorescence during the cryosectioning procedure.

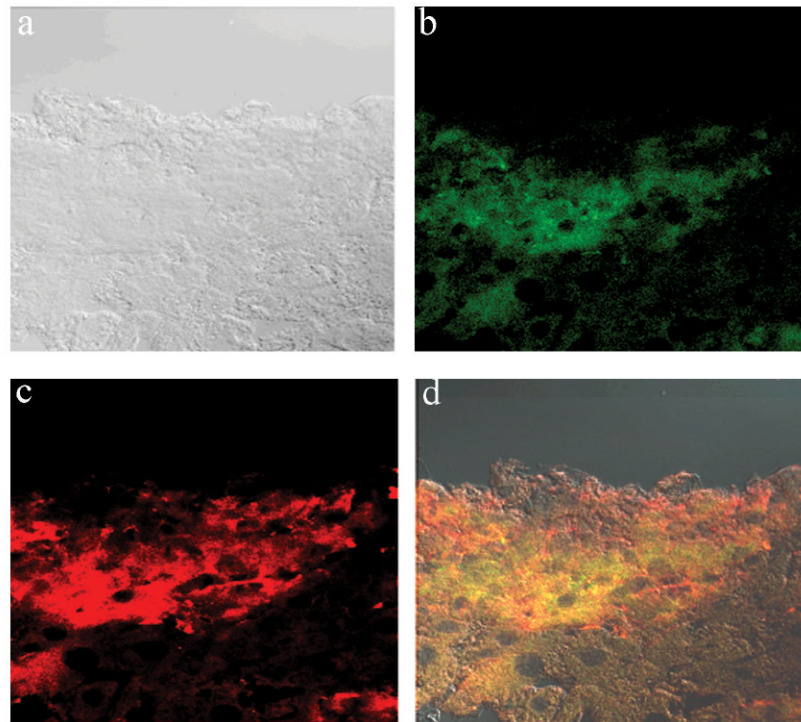


**Fig 4.** Immunofluorescence analysis of Factor IX production. Fluorescent positive areas were cryosectioned and co-immunostained for GFP (green) and Factor IX (red). Images were analyzed by confocal microscopy. (a) Light image, (b) fluorescent images, (c) overlay. Co-staining allows for identification of specific cells that may be producing factor IX (co localization of GFP+ cells with F-IX, yellow).

**TABLE 1**  
Fluorescence Stereomicroscopy as Screening Tool.

	Transplanted	Non-Transplanted
Fluorescence +	5	0
Fluorescence -	1	5
PCR +	6	0
PCR -	0	5
Total	6	5

p=0.02, Fisher exact test